Impact of macro diversity on the final throughput of a 60GHz SFN deployment

Patrick Labbé, Jeremy Gosteau and Markus Muck
Motorola Labs - Paris
Espace Technologique de Saint-Aubin
91193 Gif sur Yvette, France
Email: patrick.labbe@motorola.com

Jörg Pamp and Rens Baggen
IMST
Carl-Friedrich-Gauss-Str. 2
D-47475 Kamp-Lintfort, Germany
Email: baggen@imst.de

***Abstract*— In the framework of the IST-BROADWAY project, a hybrid WLAN system is defined working at 5GHz and 60GHz. The 60GHz band is used in order to off-load 5GHz connection for a limited time: higher throughput and better availability is achieved with the drawback of a limited coverage. This contribution presents a methodology for characterization of the available throughput over a given area based on ray-tracing simulations: exploiting a classification of the channel impulse responses (CIR) and the simulated power levels, Packet-Error-Rate (PER) simulations are performed and thus the maximum throughput for a given PER level is obtained. This proposal is applied in order to compare a single-antenna 60GHz transmission scenario (office space) to a simple Single-Frequency-Network (SFN) approach extending the number of transmit antennas to four. The results illustrate that a straightforward increase of the available number of transmit antennas may lead to destructive interference and thus to reduce performances over large parts of the considered area. Detailed evaluations are shown to be necessary in order to fully benefit from the potential of a SFN network.**

I. INTORDUCTION

In the IST-BROADWAY project [1], a hybrid dual frequency system is defined based on a tight integration of IEEE 802.11a/HIPERLAN/2 (based on the highly spectrum efficient OFDM modulation) technology at 5GHz and an innovative fully ad-hoc extension at 60GHz named HIPERSPOT. This concept extends and complements existing 5GHz broadband wireless LAN systems in the 60GHz range for providing a new solution to very dense urban deployments and hot spot coverage [2]. The resulting system guarantees nomadic terminal mobility in combination with higher capacity (achieving data rates exceeding 100Mbps). The new radio architecture will, by construction, inherently provide backward compatibility to current 5GHz WLANs (ETSI BRAN HIPERLAN/2 and IEEE 802.11a).

Propagation at 60GHz has been largely studied during the last decade. The first characterizations were published in the 90s: the context was mainly outdoor oriented, where high absorption losses are observed. This motivated its use in indoor environment. Each material and room configuration were studied and characterized in term of path loss [3]–[5]. Ray-tracing tools have been also used and calibrated to corroborate the indoor experiments so that this methodology is suitable to provide power maps and channel models with sufficient consistency [6], [7].

The first part of this study aims at providing a methodology in order to determine the maximum throughput at any position of an area over which ray-tracing data are available. Then, a specific application to this methodology is considered in the context of a 60GHz WLAN scenario: two antenna deployments are compared. This type of study helps to i) prepare the deployment of a network on a large open space, ii) find potential trade-offs between shadowed area and homogenous data-rate by tuning the emitted power, and iii) determine a reasonable number of hotspots. Both antenna configurations are analyzed with respect to the available throughput for a virtual user that can be anywhere in the room. It will take into account the propagation of 60GHz rays and their interference (quantified by ray-tracing tools), as well as their impact on the final throughput by using an abstraction of the PHY and lower MAC layers.

This paper is organized as follows. Section II states the problem and defines the different scenarii we have considered here. Then, our methodology is detailed step by step: section III presents the raw data coming from the ray-tracing tool, section IV analyzes the power repartition in the room, section V derives the channel modelization and, after presenting the PHY layer in section VI, section VII gives the final throughput estimation. Finally, section VIII summarizes this work.

II. PROBLEM STATEMENT

In this study, the layout of a typical office room (see figure 1) already used in the framework of IST-BROADWAY in order to modelize 60GHz channels [8] is defined. A wall is added in the upper left corner, in order to create a shadowed area

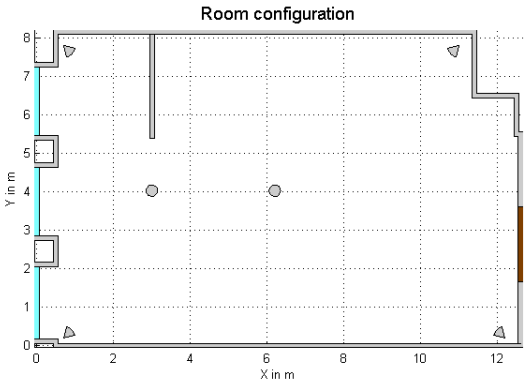

Fig. 1. Typical office room and antenna positions used to illustrate the effects of 60GHz propagation with ray-tracing tool (circles and quadrant represent omni-directional and directional antenna respectively).

for users at desk height. Please note that the wall does not reach the ceiling, which helps to include possible effects of diffraction. Two main scenarii are considered:

- Scenario 1: a single base station antenna is deployed at two different spots of a room:
  - 1a. The base station antenna is mounted on the ceiling in the centre of the room, *i.e.* users at desk height on the left side of the upper left wall do not have an unobstructed Line of Sight (LOS) link towards the base station.
  - 1b. The base station antenna is mounted on the ceiling in line with the wall, *i.e.* almost all users in the room have an unobstructed LOS link towards the base station. At system level, this base station will be used to relay the information.
- Scenario 2: four base station antennas are mounted in each corner of the room under the ceiling: they transmit the same signal, such that the entire room is covered. Each point of the room has at least one LOS link with one of the four emitters.

The total emitted power is identical for scenarii 1 and 2, but it can be tuned in order to compensate several drawbacks of a particular deployment. Two types of antennas are used for the simulations: an omnidirectional antenna in azimuth in scenario 1 and a directional antenna with a 90 degrees horizontal beamwidth, pointing at the room centre at desk height in scenario 2. Each antenna has been represented in figure 1.

In order to compare the two main scenarii, we intend to use ray-tracing simulation results in order to predict the available throughput at any spot of the room. Our approach, presented in figure 2, consists in:

- determine separately the SNR cartography over the room (derived from the raw received power data combined with the theoretical noise floor of a virtual receiver);
- extract several characteristics channel models. The channel models enable to calculate PER curves (PER as a function of a pre-determined metric, the SNR in this case), using a link simulator;
- combine these three sets of results (namely, the channel models, the SNR, and the PER curves) in order to provide the final throughput map of the room.

Several intermediate data processes are detailed below. They are in particular necessary in the concatenation of the single frequency network (SFN) information and in the filtering of the rays at each observation point (ordering and combination of rays by arrival time).

III. Ray-tracing data

The full 3D model of the ray tracing tool Wireless InSite 2.0 from Remcom Inc. is used for the simulations. This model includes an unlimited number of reflections and transmissions as well as diffraction phenomena. Two types of outputs are generated by the simulations: the received power and the Channel Impulse Response (CIR), as detailed in the following.

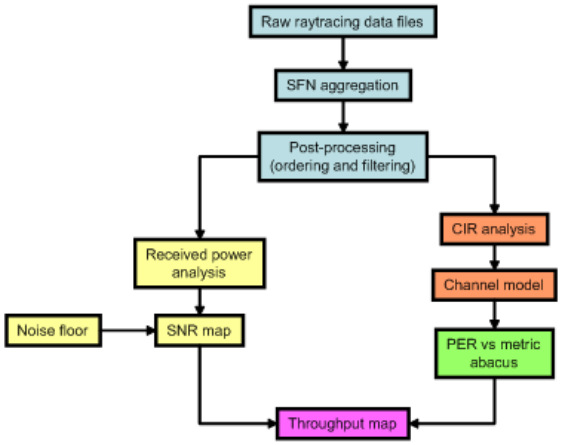

Fig. 2. Presentation of the overall methodology leading to the throughput map.

A. Received power

All fields are coherently combined (with phase). The total received power is

$$P_R = \frac{\lambda^2}{8\pi^2\eta_0}\left|\sum_{i=1}^{N_p} E_{\Theta,i}g_\Theta(\Theta_i,\Phi_i) + E_{\Phi,i}g_\Phi(\Theta_i,\Phi_i)\right|^2 \quad (1)$$

where λ is the wavelength, η_0 is the impedance of free space (377Ω), $E_{\Theta,i}$ and $E_{\Theta,i}$ are the Θ and Φ components of the electric field of the i^{th} path at the receiver point, Θ_i and Φ_i give the direction of arrival. $g_\Theta(\Theta,\Phi)$is defined by:

$$g_\Theta(\Theta,\Phi) = |G_\Theta(\Theta,\Phi)|^{\frac{1}{2}}\exp(j\Phi_\Theta) \quad (2)$$

where G_Θ is the Θ component of the receiving antenna gain, Φ_Θ is the relative phase of the Θ component of the far zone electric field. An analogous definition is used for g_Θ.

B. Channel impulse response (CIR)

The complex voltage at the feed point of the receiving antenna due to the i^{th} propagation path is proportional to

$$V_i = E_{\Theta,i}g_\Theta(\Theta_i,\Phi_i) + E_{\Phi,i}g_\Phi(\Theta_i,\Phi_i) \quad (3)$$

The complex impulse response is considered to be:

$$s_i = P_i\exp(j\Psi_i) \quad (4)$$

where P_i is the power carried by the i^{th} ray path, and Ψ_i is the phase:

$$\Psi_i = \text{atan}\left(\frac{\text{Im}(V_i)}{\text{Re}(V_i}\right) \quad (5)$$

In order to build the single frequency network, we consider that the four maps obtained for scenario 2 correspond to independent realizations of the emission. With this hypothesis, the four maps can be considered as uncorrelated; consequently, it is possible to store the rays in the same CIR as additional realization of the channel, since each measurement has been performed at the same point. Finally, each CIR (for the SFN case and the first scenario) are ordered by arrival time (for convenience sake). All rays with the same arrival time are recombined by summing the induced electrical complex fields, such that each point has a discrete ray arrival. This is important for the channel study presented in V.

IV. Received power study

The results obtained in scenario 1 are presented by figures 3(a) and 3(b). The corresponding power maps represent the power received at desk level (80cm above the floor), assuming that the omni-directional antenna is at the center of the ceiling. The colorbar indicates the power level in dBm (on the right end side). The radiation pattern decreases very slowly with the distance (less than 5dB between the center and the border of the room), except in the shadowed area. Indeed, in the upper left corner of the room, the presence of the wall decreases the power by more than 20dB. Furthermore, the concrete walls delimiting the room are responsible for a complete cancelation of the signal (the level is below the precision of our simulation tool).

The SNR is easily computed from the received power, by removing the thermal noise. The latter is a function of the temperature T (in Kelvin), the bandwidth B (in Hz), and the noise figure NF (in dB), as shown in the following equation:

$$N = 10\log_{10}\left(\frac{kT}{10^{-3}}\right) + NF + 10\log_{10}(B) \qquad (6)$$

where k is the Boltzmann constant. The noise figure is dependent on the receiver implementation and can take values of up to 10dB. Typically,

$$\text{for } B = 80 \text{ MHz}, N = -85 \text{ dBm} \qquad (7)$$

Considering the resulting SNR maps, several remarks can be made:

- in scenario 1a, the SNR received can be greatly affected by the shadowing wall;
- in all scenarii, the SNR is greater with a receiver being closer to the transmitter: this phenomenon is rather perceived in scenario 1 (where the transmitted power is higher);
- overall, scenario 2 enables a good coverage, with the drawback of a lower SNR, compared to the first scenario.

V. Modeling of 60GHz channels

The modeling of the 60GHz channels is based on the ray-tracing simulation results. These provide CIR estimates for each spot of the analyzed surface. Ideally, we should implement each CIR estimation in the link level simulation environment and perform corresponding packet error rate (PER) simulations in order to evaluate the available throughput. Due to the large number of points, we choose to limit the simulations to a set of four typical CIRs. As a main characteristic of the different CIRs, we choose to define four classes of channel delay spreads (see below) and to link the CIR of each spot to the closest channel in this set. Since the delay spread is a main criterion for the PER simulation results, this approach will guarantee a broad scope of channels with different performance properties.

The analysis is first based on specific a study of the room repartition: different delays are experienced by the CIR on each point, for each scenario. For that purpose, we set a threshold (e.g. -10dB) below which the taps will not be considered as relevant. Note that, by definition, the first tap has a null delay and a power equal to 0dB. Initially, we choose

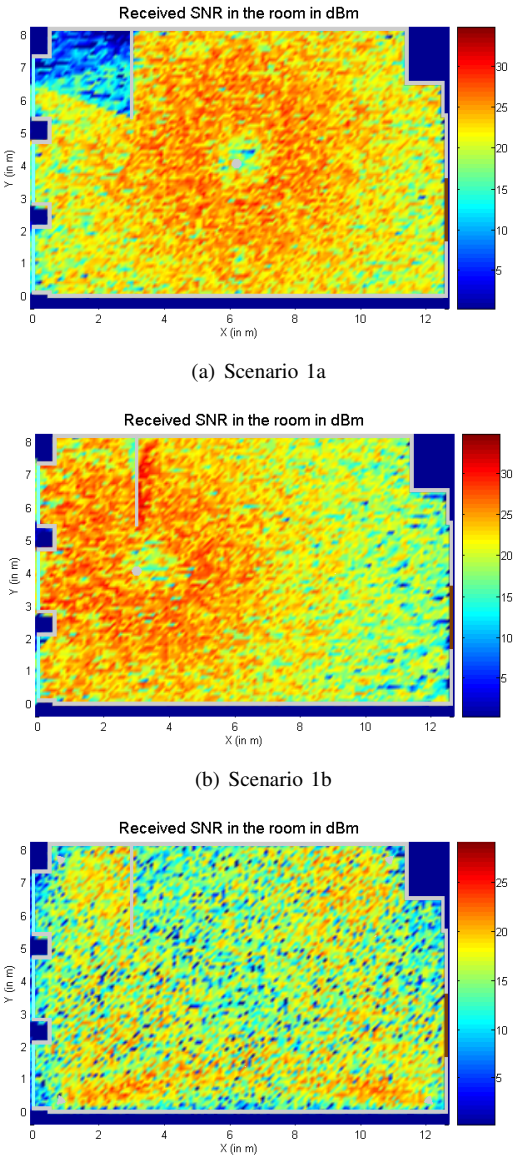

(a) Scenario 1a

(b) Scenario 1b

(c) Scenario 2

Fig. 3. SNR map of the room for all scenarii with an SNR scale ranging from 0 to 35dB.

to discriminate four different channels along the room. The question is to determine the number of taps (maximum delay) for each of the four channels. The following methodology is applied for a given scenario (e.g. 1a), we determine the number of taps for each channel in order to associate with it 25% of the points in the room. Hence, the channel models are evenly used over the room.

For instance, knowing that one tap corresponds to 4.2ns, the largest delay is approximately 100ns, corresponding to 20 taps or a similar value. Therefore, we have a vector used for the model definition [0 5 10 15], indicating that:

- from tap 0 to tap 5 (channel type 1): all the taps from 0 to 4 are above -10dB, the taps after 5 are below;
- from tap 0 to tap 9 (channel type 2): all the taps from 0 to 9 are above -10dB, the taps after 10 are below;
- from tap 0 to tap 14 (channel type 3): all the taps from 0 to 14 are above -10dB, the taps after 15 are below;

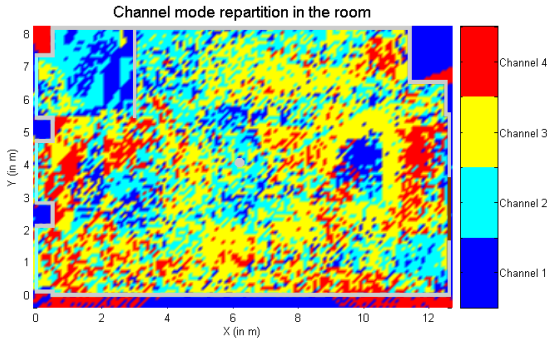

(a) Scenario 1a

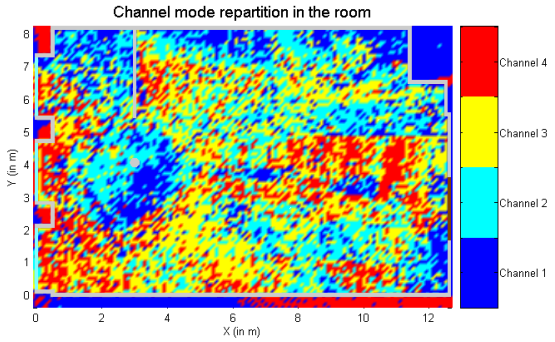

(b) Scenario 1b

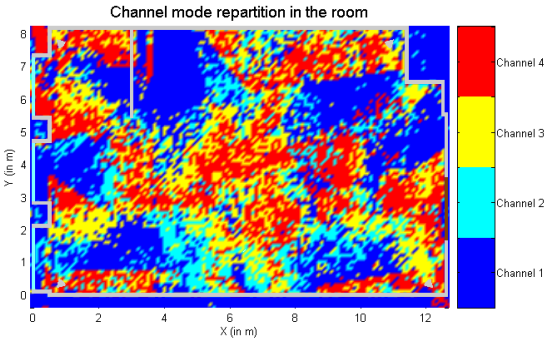

(c) Scenario 2

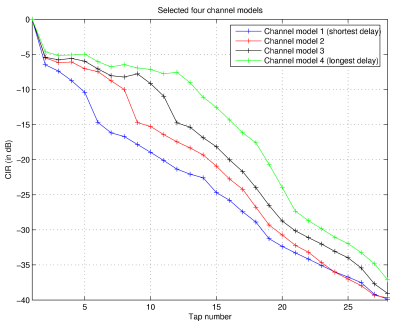

(d) CIR of selected 4 channel models

Fig. 4. Channel type map of the room for all scenarii.

- from tap 15 onwards (channel type 4): all the taps are below -10dB.

In order to determine this vector of the model definition and the threshold, an optimization program is run. We choose one of the offered solutions: threshold=-10dB, model definition= [0 6 9 13]. The result is presented by figure 4. This model is also suitable for scenarii 1b and 2.

VI. PHY LAYER SIMULATIONS

The throughput analysis is based on link level simulation results: all available PHY modes are simulated; then, we consider the PER simulation results at the SNR level indicated by the ray-tracing evaluation.

The link level simulations have been run for the constellations BPSK, QPSK, QAM-16 and QAM-64, each based on the code rate 1/2, 3/4 and 9/16 of a standard convolutional encoder with constraint length K=7 and coding polynomials 133oct and 171oct. The packet sizes were fixed to 72 OFDM symbols for BPSK and QPSK simulations and to 92 OFDM symbols for QAM-16 and QAM-64. Each simulation was run over 1500 iterations.

VII. FINAL THROUGHPUT

Now, the last information that remains is the mode to be used for each position in the room: the knowledge of the mode is required to select the adequate PER vs. SNR curve, and therefore enables the computation of the adequate throughput (expressed as a function of the PER). The following methodology is used to compute the correct mode: for a given SNR, we maximize the throughput available on top of the PHY. This throughput is expressed as

$$\rho = bit\_rate(mode).(1 - PER(mode)) \quad (8)$$

where the bit_rate and the throughput ρ are expressed in Mbit/s.

The throughput for each of the simulated modes is plotted on figure 5(d) for a given channel model. This graph illustrates that there are SNR ranges where a given mode maximizes the throughput (for a given channel model). Quite naturally, we will use the modes (and their associated PER curves) maximizing the throughput for a given SNR and channel model. It corresponds to the use of an *ideal* link adaptation algorithm. Figure 5(d) also proves that some modes are useless and should not be used: this is the case for BPSK 9/16 and BPSK 3/4, or QAM64 1/2.

Using this methodology, a new map of the room can be plotted in terms of throughput on top of the PHY layer. The results are presented on the three sub-figures of figure 5.

One can draw similar conclusions on figures 3, with respect to the analysis of figures 5. In scenario 2, two aspects are remarkable: the homogeneity of the offered throughput, and the presence of important drops (less than 40Mbit/s) close to areas of good throughput (more than 120Mbit/s).

VIII. CONCLUSION

In this study, we successively derived the SNR map as well as several channel models (relevant of 60GHz behaviors) from the ray-tracing data collected in an arbitrary defined room. We finally aggregated all data in the link level simulator in

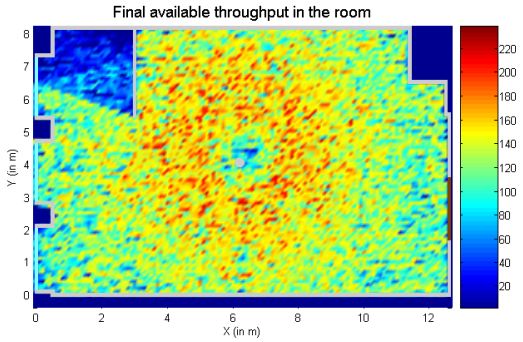

(a) Scenario 1a

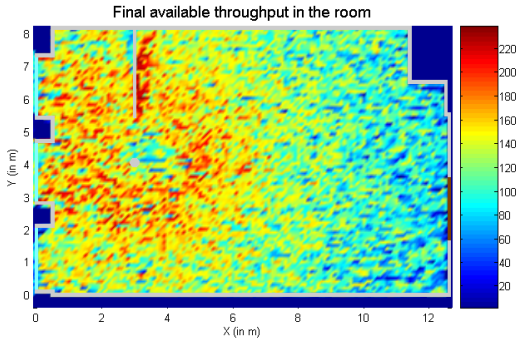

(b) Scenario 1b

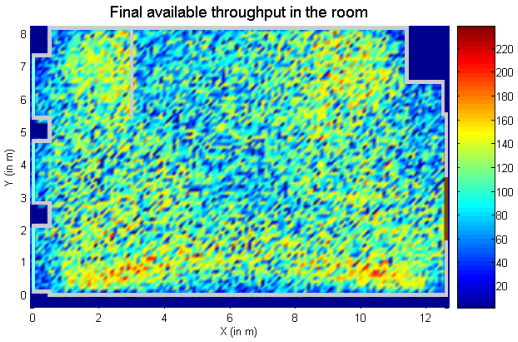

(c) Scenario 2

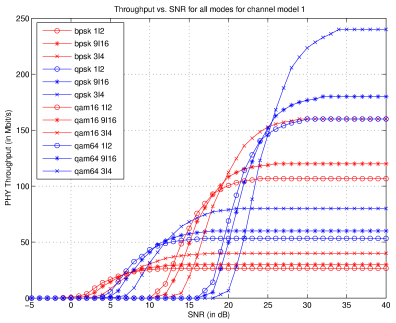

(d) Throughput vs. SNR for all used modes

Fig. 5. Throughput map of the room for all scenarii, with a throughput scale ranging from 0 to 240Mbit/s.

order to exhibit the available throughput on each point of the room with a theoretical maximum throughput of 240Mbit/s (corresponding to 80MHz channel).

The data-rate map reveals that the interference at 60GHz is highly penalizing in a multi hotspot deployment. It can be observed that cancelation points are very close to each other (due to the short wavelength at 60GHz) and that the overall throughput remains lower than in the case of a single hotspot deployment as long as the channel is distorted by other feed points (around 140MBit/s in most case instead of 200MBit/s in majority in the single hotspot configuration). On the opposite, a single hotspot installation is not exempt of a shadowed area as observed in scenario 1a.

Hence, instead of deploying a multi hotspots system (penalizing all the covered room), it would be better to move the main hotspot in order to cover the room according to the optical sense or take benefit of the shadowed area to deploy the hotspot so that they could not interfere each other. As for future activities, the methodology can still be further developed with the use of other metrics than the SNR that might be more relevant to discriminate channel models.

ACKNOWLEDGMENT

The works presented are supported by the European Commission through the research project BroadWay and the authors are gratefully thank all the partners involved.

REFERENCES

[1] M. de Courville, S. Zeisberg, M. Muck, and J. Schoenthier. BroadWay - the way to broadband access at 60GHz. In *International Conference on Telecommunication*, Beijing, China, June 2002.

[2] P.F.M. Smulders. Exploiting the 60GHz band for local wireless multimedia acess: prospects and future directions. *IEEE communications magazine*, pages 141–146, January 2002.

[3] N. Moraitis and P. Constantinou. Indoor channel measurements and characterization at 60GHz for wireless Local Area Network applications. *IEEE Transactions on Antennas and Propagation*, 52(12):3180–3189, December 2004.

[4] H. Xu, V. Kukshya, and T.S. Rappaport. Spatial and temporal characteristics of 60GHz indoor channels. *IEEE Journal on selected areas in communications*, 20(3):620–630, April 2002.

[5] L. Correia and P.O. Frances. Transmission and isolation of signals in buildings at 60GHz. *PIMRC'95, IEEE International Symposium on 'Wireless: Merging onto the Information Superhighway'*, 3:1031–1034, September 1995.

[6] D. Dardari, L. Minelli, V. Tralli, and O. Andrisano. Fast ray-tracing characterization of indoor propagation channels at 60GHz. *IEEE 47th Vehicular Technology Conference*, pages 989–993, May 1997.

[7] P.F.M. Smulders and L.M. Correia. Characterisation of propagation in 60GHz radio channels. *Electronics & communication engineering journal*, pages 73–80, April 1997.

[8] Markus Muck, Jens Schönthier, and Kai-Uwe Schmidt. The 60GHz channels and its modelling. Technical report, Deliverable D7R3 Annex 1 of IST-BROADWAY project IST-2001-32686, available at `http://www.ist-broadway.org`, 2004.